Enhanced high temperature performance of LiMn$_2$O$_4$ coated with Li$_3$BO$_3$ solid electrolyte

LIU JINLIAN[1], **WU XIANMING**[1,2,*], **CHEN SHANG**[1,2], **LIU JIANBEN**[1,2] **and HE ZEQIANG**[1,2]

[1]College of Chemistry and Chemical Engineering, Jishou University, Jishou 416000, China
[2]Xiangxi Ores and New Materials Development and Service Centre, Jishou 416000, China

Abstract. Cathode material, LiMn$_2$O$_4$, was synthesized by solid-state reaction followed by surface coating of Li$_3$BO$_3$ solid electrolyte. Structure and electrochemical performance of the prepared powders were characterized by X-ray diffraction, scanning electron microscopy, cyclic voltammetry, electrochemical impedance spectroscopy and galvanostatic charge–discharge techniques, respectively. Results show that Li$_3$BO$_3$ coated LiMn$_2$O$_4$ has similar X-ray diffraction patterns as LiMn$_2$O$_4$. The discharge specific capacities of LiMn$_2$O$_4$ coated with 0·1, 0·3 and 0·6 wt% Li$_3$BO$_3$ are 123·3, 118·2 and 110 mAh/g, respectively, which is slightly smaller than that of 124·4 mAh/g for LiMn$_2$O$_4$. However, the capacity retention of Li$_3$BO$_3$ coated LiMn$_2$O$_4$ is at least 5·6 and 7·6% higher than LiMn$_2$O$_4$ when cycled at room temperature and 55 °C, respectively. Li$_3$BO$_3$ coated LiMn$_2$O$_4$ shows much better cycling behaviours than LiMn$_2$O$_4$.

Keywords. Lithium ion battery; lithium manganese oxide; coating; solid-state method.

1. Introduction

LiCoO$_2$ was widely used as cathode material for lithium ion battery because of its excellent electrochemical properties. However, this material has the drawbacks of high cost and toxicity of cobalt (Lee *et al* 2007; Ruffo *et al* 2009; Li *et al* 2011). Spinel LiMn$_2$O$_4$ was a promising candidate material for lithium ion battery due to its high voltage, non-toxicity, low cost, environmental friendliness and safety. However, LiMn$_2$O$_4$ exhibits serious capacity fading during charge and discharge cycling, especially at elevated temperature, which has been ascribed to the following factors: (i) dissolution of Mn^{2+}; (ii) Jahn–Teller distortion of Mn^{3+} ions and (iii) decomposition of electrolyte solution on LiMn$_2$O$_4$ electrode (Sun 2000; Chung and Kim 2004; Wu *et al* 2005; Wei *et al* 2009).

In order to suppress the dissolution of manganese, surface coating of LiMn$_2$O$_4$ with various protective layers as Cr$_2$O$_3$ (Sahan *et al* 2010), CoO (Arumugam and Kalaignan 2010), CeO$_2$ (Ha *et al* 2007; Arumugam and Kalaignan 2010), ZnO (Tu *et al* 2007), ZrO$_2$ (Lim and Cho 2008), MgO (Gnanaraj *et al* 2003), Al$_2$O$_3$/CuO (Lee *et al* 2004) and AlPO$_4$ (Shi *et al* 2010) have been employed. However, these coating materials are not lithium ion conductors which can form barriers to the movement of lithium ions. Considering that Li$_3$BO$_3$ is a good kind of solid electrolyte with excellent lithium ionic conductivity, the coating of Li$_3$BO$_3$ on the surface of LiMn$_2$O$_4$ is attempted in this work to improve the electrochemical property of LiMn$_2$O$_4$.

2. Experimental

Stoichiometric of lithium carbonate and electrolytic manganese dioxide were fully mixed in a mortar. Then the mixture was calcined at 750 °C for 24 h in air at a heating rate of 5 °C/min followed by natural cooling to ambient temperature to obtain LiMn$_2$O$_4$ powders.

Li$_3$BO$_3$-coated LiMn$_2$O$_4$ powders were prepared as follows: LiCH$_3$COO·2H$_2$O and H$_3$BO$_3$ in the molar ratio of 3:1 were dissolved in ethanol and stirred for 1 h to obtain Li$_3$BO$_3$ precursor solution. LiMn$_2$O$_4$ powders were added slowly to the precursor solution and stirred vigorously at 85 °C for 2 h until the solvent was completely evaporated. The dried powders were finally annealed at 600 °C for 10 h in air to obtain LiMn$_2$O$_4$ coated with Li$_3$BO$_3$ of 0, 0·1, 0·3 and 0·6 wt%, respectively.

Structure and surface morphology of the products were characterized by X-ray diffraction and scanning electron microscopy. Electrochemical measurements were conducted through a coin type cell (CR2025) with lithium metal as both counter and reference electrodes and 1 mol L^{-1} ethylene carbonate (LiPF$_6$/EC)–dimethyl carbonate (DMC) solution as electrolyte. Composite cathodes were fabricated as follows: LiMn$_2$O$_4$ or Li$_3$BO$_3$-coated LiMn$_2$O$_4$, carbon black and polyvinylidene fluoride (PVDF) in the weight ratio of 8:1:1 were mixed in *n*-methyl pyrrolidinone followed by a vacuum drying at 120 °C for 10 h. The entire cell was assembled in an argon-filled glove box. Galvanostatic charge–discharge experiments were conducted between 4·3 and 3·0 V at the rate of 0·2 °C at room and elevated temperatures. Cyclic voltammetry was measured between 3·3 and 4·6 V with a potential scan rate of 50 μV/s. Electrochemical impedance

---

*Author for correspondence (xianmingwu@163.com)

spectroscopy was carried out in the frequency range of 0·1 Hz–100 kHz with 10 mV amplitude of a.c. potential.

3. Results and discussion

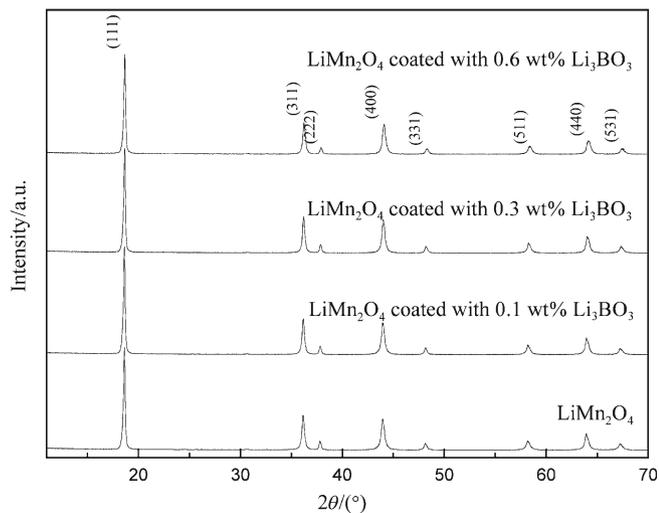X-ray diffraction patterns of $LiMn_2O_4$ and $LiMn_2O_4$ coated with different weight percentages of Li_3BO_3 are shown in figure 1. As seen in the figure, (111), (311), (222), (400), (331), (511), (440) and (531) diffraction peaks were observed and the patterns of all powders are similar, indicating that the surface modified powders are the cubic spinel structure. There are no significant diffraction differences between $LiMn_2O_4$ and Li_3BO_3 coated $LiMn_2O_4$, suggesting that coating of Li_3BO_3 on $LiMn_2O_4$ does not affect the structure of $LiMn_2O_4$.

Figure 1. X-ray diffraction patterns of $LiMn_2O_4$ and $LiMn_2O_4$ coated with different weight percentages of Li_3BO_3.
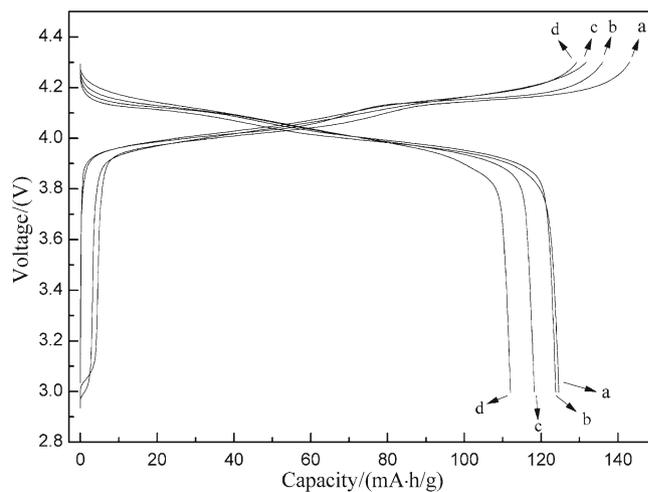

Figure 3. Charge–discharge curves of $LiMn_2O_4$ and $LiMn_2O_4$ coated with different weight percentages of Li_3BO_3.

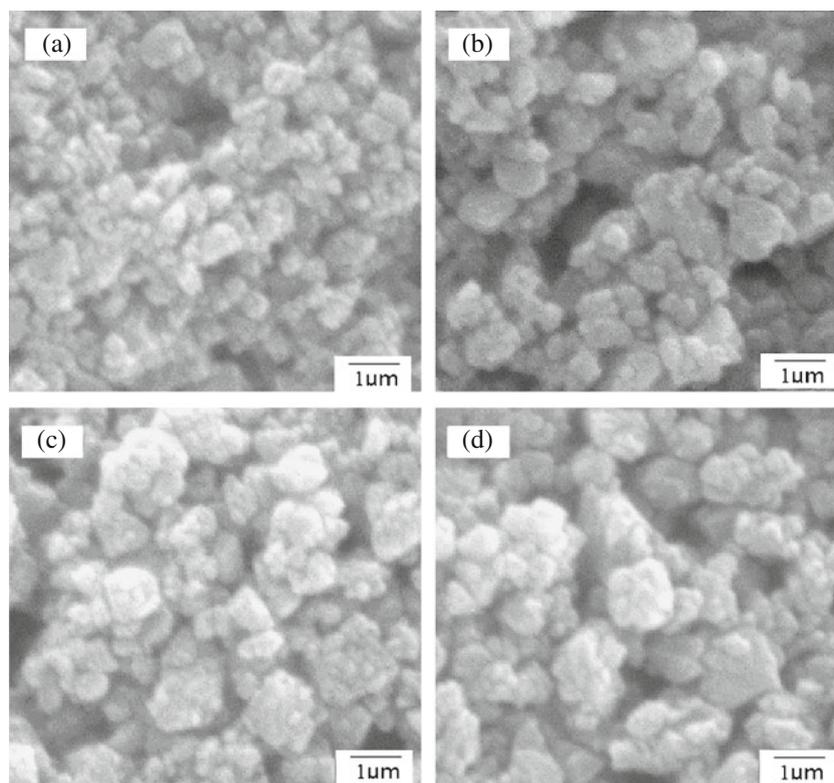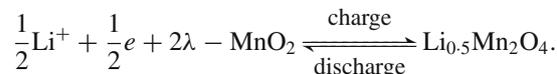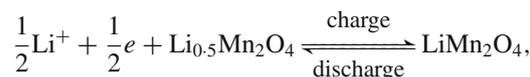**Figure 2.** Scanning electron micrographs of $LiMn_2O_4$ and $LiMn_2O_4$ coated with different weight percentages of Li_3BO_3: (**a**) 0 wt%, (**b**) 0·1 wt%, (**c**) 0·3 wt% and (**d**) 0·6 wt%.

The scanning electron micrographs of $LiMn_2O_4$ and $LiMn_2O_4$ coated with different weight percentages of Li_3BO_3 are shown in figure 2. As observed in the figure, the particles of all powders are uniform. The powders of $LiMn_2O_4$ and $LiMn_2O_4$ coated with different weight percentages of Li_3BO_3 show similar particle shape. Similar particle shape of $LiMn_2O_4$ and $LiMn_2O_4$ coated with different weight percentages of Li_3BO_3 can be attributed to the low mass coating of Li_3BO_3 (<1 wt%). However, the particle agglomeration of Li_3BO_3 coated $LiMn_2O_4$ becomes slightly more severe with the increase in coating of Li_3BO_3 and the particle corner and border of the Li_3BO_3 coated $LiMn_2O_4$ powders become less clear compared with that of the uncoated $LiMn_2O_4$.

The galvanostatic charge–discharge curves of $LiMn_2O_4$ and Li_3BO_3 coated $LiMn_2O_4$ conducted at room temperature are shown in figure 3. As observed in the figure, both charge and discharge curves of all samples exhibit two clear voltage plateaus in the potential regions of 4 and 4·1 V, which are characteristic of $LiMn_2O_4$. Two voltage plateaus indicate that both the intercalation and de-intercalation of lithium ions proceed in two stages, which can be written as the following two reversible reactions:

$$\frac{1}{2}Li^+ + \frac{1}{2}e + Li_{0.5}Mn_2O_4 \underset{\text{discharge}}{\overset{\text{charge}}{\rightleftharpoons}} LiMn_2O_4,$$

$$\frac{1}{2}Li^+ + \frac{1}{2}e + 2\lambda - MnO_2 \underset{\text{discharge}}{\overset{\text{charge}}{\rightleftharpoons}} Li_{0.5}Mn_2O_4.$$

The figure also shows that initial discharge specific capacity of $LiMn_2O_4$ is 124·4 mAh/g, while those for the $LiMn_2O_4$ coated with 0·1, 0·3 and 0·6 wt% Li_3BO_3 are 123·3, 118·2 and 110 mAh/g, respectively. The specific capacity of Li_3BO_3 coated $LiMn_2O_4$ is slightly smaller than $LiMn_2O_4$.

Cycling behaviours of $LiMn_2O_4$ and Li_3BO_3 coated $LiMn_2O_4$ cycled 40 times at room temperature and 55 °C are shown in figure 4. For the samples cycled at room temperature, the discharge specific capacity of $LiMn_2O_4$ decreases from 124·4 to 105·8 mAh/g with the capacity retention of 85·3%. While the specific capacity of $LiMn_2O_4$ coated with 0·1, 0·3 and 0·6 wt% Li_3BO_3 decreases from 123·3, 118·2, 110 to 112·5, 108·7 and 104·3 mAh/g with capacity retention of 90·9, 92·0 and 93·1%, respectively. The capacity retention of Li_3BO_3 coated $LiMn_2O_4$ is much higher than $LiMn_2O_4$. For the samples cycled at 55 °C, the discharge specific capacity of $LiMn_2O_4$ decreases from 123·29 to 96·5 mAh/g with a capacity retention of 78·3%, while the specific capacity of $LiMn_2O_4$ coated with 0·1, 0·3 and 0·6 wt% Li_3BO_3 decreases from 121·1, 119·3 and 115·2 mAh/g to 103·9, 104·5 and 104·4 mAh/g with a capacity retention of 85·9, 87·8 and 90·6%, respectively which is also much higher than $LiMn_2O_4$. The results indicate that the coating of Li_3BO_3 can greatly improve the cycling behaviour of $LiMn_2O_4$, especially at elevated temperature.

One main reason of the capacity fading of $LiMn_2O_4$ during cycling is the dissolution of manganese in the electrolyte, which becomes faster with increase in temperature.
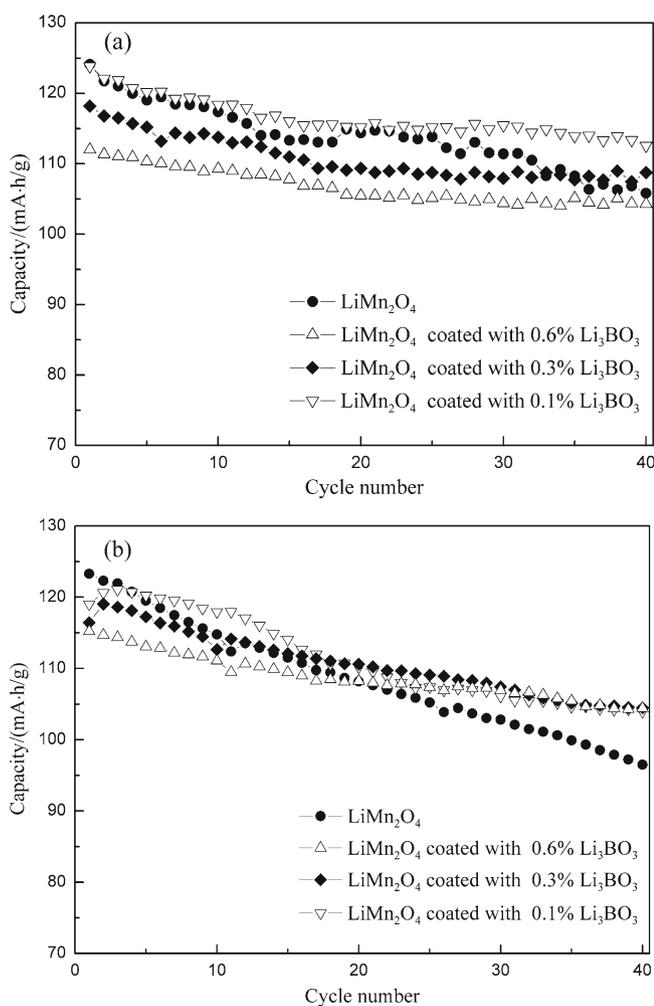

Figure 4. Cycling behaviours of $LiMn_2O_4$ and Li_3BO_3 coated $LiMn_2O_4$ cycled (**a**) at room temperature and (**b**) 55 °C.
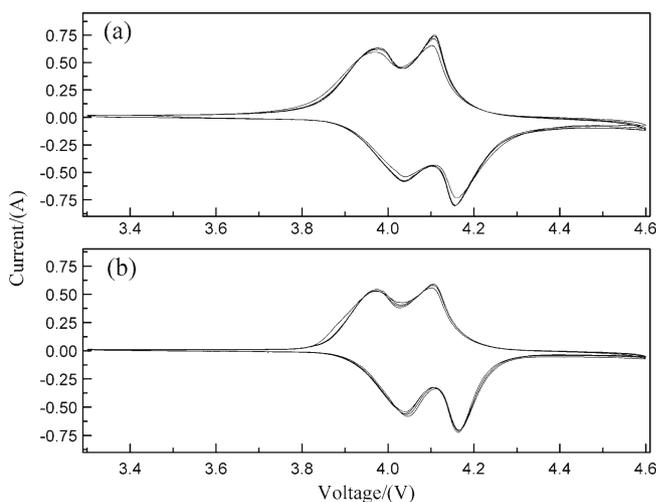

Figure 5. First to fourth cyclic voltammogram of (**a**) $LiMn_2O_4$ and (**b**) $LiMn_2O_4$ coated with 0·1 wt% Li_3BO_3.

Aurbach (2000) confirmed that HF generated during cycling in $LiPF_6$-based electrolyte was responsible for the dissolution of manganese. Wang *et al* (2000) proposed the following chemical reactions:
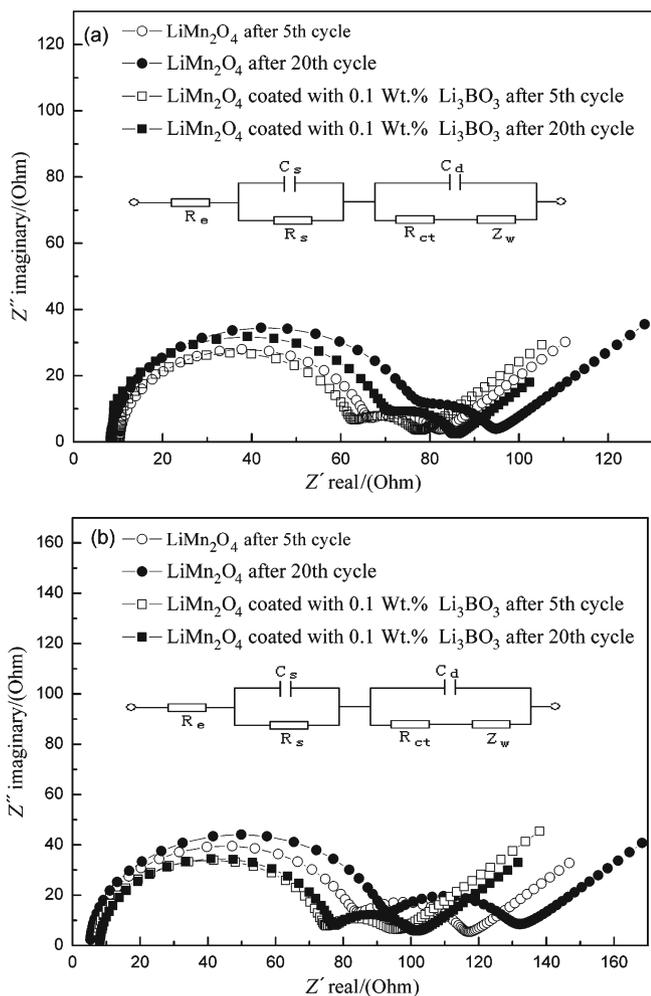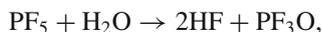
$$LiPF_6 \rightarrow LiF + PF_5,$$

$$PF_5 + H_2O \rightarrow 2HF + PF_3O,$$

$$2LiMn_2O_4 + 4H^+ \rightarrow 3\lambda - MnO_2 + Mn^{2+} + 2Li^+ + 2H_2O.$$

Figure 6. Nyquist plots of $LiMn_2O_4$ and $LiMn_2O_4$ coated with 0·1 wt% Li_3BO_3 after desired cycles: (**a**) room temperature and (**b**) elevated temperature (55 °C).

From the above reactions, it is known that acid is self-catalytic and HF is regenerated by the reaction of water with PF_6. These reactions result in the dissolution of electrode material during cycling, leading to relatively poor cycling performance. Coating of Li_3BO_3 on the surface of $LiMn_2O_4$ has little influence on the movement of lithium ion because Li_3BO_3 is a kind of lithium ion conductor. However, it can reduce the contact area of $LiMn_2O_4$ electrode/electrolyte interface or even separate the direct contact of electrode material with liquid electrolyte, which reduces the dissolution of manganese and the oxidation of electrolyte, resulting in better cycling performance.

The first to fourth cyclic voltammograms of $LiMn_2O_4$ and $LiMn_2O_4$ coated with 0·1 wt% Li_3BO_3 are displayed in figure 5. As seen in the figure, both samples show two couples of redox peaks at around 3·98 and 4·13 V, the split of the redox peaks into two couples indicates that electrochemical intercalation and de-intercalation reactions of lithium ion proceed in two steps. Intensity of the redox peaks for Li_3BO_3 coated $LiMn_2O_4$ is smaller than $LiMn_2O_4$, yet much more steady than the latter, which implies that Li_3BO_3 modified $LiMn_2O_4$ has smaller discharge capacity and better reversibility than $LiMn_2O_4$.

Electrochemical impedance spectra and equivalent circuits of $LiMn_2O_4$ and $LiMn_2O_4$ coated with 0·1 wt% Li_3BO_3 are shown in figure 6. The measurements were carried out at open circuit voltage of 4·1 V and as a function of cycle number at room temperature and 55 °C. The figure shows that impedance spectra composed of two semicircles in high and medium frequency zone and a line inclined at an angle of 45° to the real axis in the low frequency range. The semicircle in the high frequency range is caused by the formation of solid electrolyte interface film (SEI film). The middle frequency semicircle is associated with the 'charge transfer reactions' at interface of SEI film and oxide electrode, which corresponds to charge–discharge resistance. The inclined line in the low frequency range is attributed to 'Warburg impedance' that is associated with lithium diffusion through the oxide electrode. In the equivalent circuit, R_e is the electrolyte resistance, R_s the surface film resistance, R_{ct} the charge-transfer resistance, C_s the surface film capacitance, C_d the double layer capacitance and Z_w the Warburg impedance. From these electrochemical impedance spectra and equation of $\omega RC = 1$, the values of R_s and R_{ct} after

Table 1. R_s and R_{ct} values of $LiMn_2O_4$ and $LiMn_2O_4$ coated with Li_3BO_3 of 0·1 wt% after different cycles at room and elevated temperatures (55 °C).

	$LiMn_2O_4$/room temperature	Coated $LiMn_2O_4$/ room temperature	$LiMn_2O_4$/55 °C	Coated $LiMn_2O_4$/55 °C
R_s (after 5th cycle)/Ω	55·5	53·5	77·9	67·4
R_s (after 20th cycle)/Ω	67·7	62·8	87·2	68·7
R_{ct} (after 5th cycle)/Ω	14·4	13·6	30·6	18·4
R_{ct} (after 20th cycle)/Ω	16·3	14·3	35·4	22·0
Z_w (after 5th cycle)/Ω	11·3	10·9	12·6	12·1
Z_w (after 20th cycle)/Ω	13·6	12·1	19·0	15·5

5th and 20th cycles are determined in table 1. As seen in the table, after cycling 5 and 20 times at room temperature and 55 °C, R_{ct} of Li$_3$BO$_3$ coated LiMn$_2$O$_4$ changes from 13·6 to 14·3 Ω and 18·4 to 22·0 Ω, respectively. While those of LiMn$_2$O$_4$ change from 14·4 to 16·3 Ω and 30·6 to 35·4 Ω. R_{ct} changes of Li$_3$BO$_3$ coated LiMn$_2$O$_4$ are smaller than those of LiMn$_2$O$_4$. Variation of R_s shows similar tendency as R_{ct}. The results show that coating of appropriate amount of Li$_3$BO$_3$ on LiMn$_2$O$_4$ can reduce SEI and charge-transfer resistance and suppress the reaction between electrode materials and electrolyte.

4. Conclusions

Spinel LiMn$_2$O$_4$ was synthesized by solid-state reaction and coated with Li$_3$BO$_3$. Li$_3$BO$_3$ coated LiMn$_2$O$_4$ has similar X-ray diffraction patterns as LiMn$_2$O$_4$. The discharge specific capacity of LiMn$_2$O$_4$ coated with 0·1, 0·3 and 0·6 wt% Li$_3$BO$_3$ are 123·3, 118·2 and 110 mAh/g, respectively, which is slightly smaller than LiMn$_2$O$_4$. However, the capacity retention of Li$_3$BO$_3$ coated LiMn$_2$O$_4$ are at least 5·6 and 7·6% higher than LiMn$_2$O$_4$, when cycled at room temperature and 55 °C, respectively. The cyclic voltammetry shows that intensity of the redox peaks for Li$_3$BO$_3$ coated LiMn$_2$O$_4$ is smaller than LiMn$_2$O$_4$, yet much more steady than the latter. Electrochemical impedance spectroscopy shows that the coating of appropriate amount of Li$_3$BO$_3$ on LiMn$_2$O$_4$ can reduce SEI and charge-transfer resistance and suppress the reaction between electrode materials and electrolyte.

References

Arumugam D and Kalaignan P G 2010 *Electrochim. Acta* **55** 8709
Aurbach D 2000 *J. Power Sources* **89** 206
Chung K Y and Kim K B 2004 *Electrochim. Acta* **49** 3327
Gnanaraj J S, Pol V G, Gedanken A and Aurbach D 2003 *Electrochem. Commun.* **5** 940
Ha H W, Yun N J and Kim K 2007 *Electrochim. Acta* **52** 3236
Lee J G, Kim T G and Park B 2007 *Mater. Res. Bull.* **42** 1201
Lee S W, Kim K S, Lee K L, Moon H S, Kim H J, Cho B W, Cho W I and Park J W 2004 *J. Power Sources* **130** 233
Li J L, Daniel C and Wood D 2011 *J. Power Sources* **196** 2452
Lim S H and Cho J 2008 *Electrochem. Commun.* **10** 1478
Ruffo R, Wessells C, Huggins R A and Cui Y 2009 *Electrochem. Commun.* **11** 247
Sahan H, Goktepe H, Patat S and Ulgen A 2010 *Solid State Ionics* **181** 1437
Shi J Y, Yi C W and Kim K 2010 *J. Power Sources* **195** 6860
Sun Y K 2000 *Electrochem. Commun.* **2** 6
Tu J, Zhao X B, Xie J, Cao G S, Zhuang D G, Zhu T J and Tu J P 2007 *J. Alloys Compd.* **432** 313
Wang E, Ofer D, Bowden W, Iltchev N, Moses R and Brandt K 2000 *J. Electrochem. Soc.* **147** 4023
Wei Y J, Nikolowski K, Zhan S Y, Ehrenberg H, Oswald S, Chen G, Wang C Z and Chen H 2009 *Electrochem. Commun.* **11** 2008
Wu H C, Guo Z Z, Wen H P and Yang M H 2005 *J. Power Sources* **146** 736